Anderson localization of classical waves in weakly scattering metamaterials

Ara A. Asatryan[1], Sergey A. Gredeskul[2,3], Lindsay C. Botten[1], Michael A. Byrne[1],
Valentin D. Freilikher[4], Ilya V. Shadrivov[3], Ross C. McPhedran[5], and Yuri S. Kivshar[3]

[1] Department of Mathematical Sciences and Centre for Ultrahigh-bandwidth Devices for Optical Systems (CUDOS),
University of Technology, Sydney, NSW 2007, Australia
[2] Department of Physics, Ben Gurion University of the Negev, Beer Sheva, 84105, Israel
[3] Nonlinear Physics Center and CUDOS, Australian National University, Canberra, ACT 0200, Australia
[4] Department of Physics, Bar-Ilan University, Raman-Gan, 52900, Israel
[5] School of Physics and CUDOS, University of Sydney, Sydney, NSW 2006, Australia

We study the propagation and localization of classical waves in one-dimensional disordered structures composed of alternating layers of left- and right-handed materials (mixed stacks) and compare them with structures composed of different layers of the same material (homogeneous stacks). The main characteristic of the transport is the transmission length, which coincides with the localization and ballistic lengths in the localized and ballistic regime respectively. For weakly scattering layers, we have developed an effective analytical approach and have calculated the transmission length within a wide region of the input parameters. This enables us to describe in a unified way the localized and ballistic regimes as well as the crossover between them. When both refractive index and layer thickness of a mixed stack are random, the transmission length in the long-wave range of the localized regime exhibits a quadratic power wavelength dependence with the different coefficients of proportionality for mixed and homogeneous stacks. Moreover, the transmission length of a mixed stack differs from reciprocal of the Lyapunov exponent of the corresponding infinite stack. In the ballistic regime, the transmission length of a mixed stack for a particular realization is always a strongly fluctuating quantity, while in a homogeneous stack, it fluctuates only in the near long-wave region. In the far long-wave part of ballistic region, the transmission length is practically non-random, and the stack becomes effectively uniform. The crossover region from the localization to the ballistic regime is relatively narrow for both M- and H-stacks. In mixed stacks with only refractive-index disorder, Anderson localization at long wavelengths is substantially suppressed, with the localization length growing with wavelength much faster than for homogeneous stacks. The crossover region becomes essentially wider and transmission resonances appear only in much longer stacks. The effects of absorption on the one-dimensional transport and localization have also been studied, both analytically and numerically. Specifically, it is shown that the crossover region is particularly sensitive to losses, so that even small absorption noticeably suppresses frequency dependent oscillations in the transmission length. All theoretical predictions are in an excellent agreement with the results of numerical simulations.

PACS numbers: 42.25.Dd,42.25.Fx

I. INTRODUCTION

Metamaterials are artificial structures having negative refractive indices for some wavelengths [1]. While natural materials having such properties are not known, Pendry, in his famous paper [2] which sought concrete ways of fabricating artificial metamaterials, triggered the rapidly increasing interest in the topic. Over the past decade, the physical properties of these structures, and their possible applications in modern optics and microelectronics, have received considerable attention (see e.g. [4–6]). The reasons for such interest are their unique physical properties, their ability to overcome the diffraction limit [1, 2], and their potential role in cloaking [7], the suppression of spontaneous emission rate [8], and the enhancement of quantum interference [9], etc.

Until recently, most studies considered only ideal systems and did not address the possible effects of disorder. However, real metamaterials are always disordered, at least, in part, due to fabrication errors. Accordingly, the study of disordered metamaterials is not just an academic question but is also relevant to their application. The first step in this direction was made in Ref. [10] where it was shown that the presence of a single defect led to the appearance of a localized mode. A metamaterial with many point-like defects was considered in Ref. [11] where it was demonstrated that even a weak microscopic disorder might lead to a substantial suppression of wave propagation through metamaterial over a wide frequency range.

The next steps in this direction focused on the study of localization in metamaterials. Anderson localization is one of the most fundamental and fascinating phenomena of the physics of disorder. Predicted in the seminal paper [12] for spin excitations, it was extended to the case to electrons and other one-particle excitations in solids, as well as to electromagnetic waves (see, e.g., Refs. [13, 14, 16, 18]), becoming a paradigm of modern physics.

Anderson localization results from the interference of multiply scattered waves, manifesting itself in a most pronounced way in one-dimensional systems [14, 16] in which all states become localized [19], so that the envelope of

each state decays exponentially away from a randomly located localization centre [14]. The rate of this decay is non-random and is called tghe Lyapunov exponent, γ, the reciprocal of which determines the size of the area of localization.

In a finite, but sufficiently long, disordered sample, the localization manifests itself in the fact that the frequency dependent transmission amplitude is (typically) an exponentially decreasing function of the sample size. The average of this decrement is a size-dependent quantity, whose inverse is termed as *transmission length, l_N*. In the limit as the sameple becomes of infinite length, the decrement tends to a constant non-random value. The reciprocal of this value determines another characteristic spatial scale of the localized regime, which is the *localization length, l*. It is commonly accepted in both the solid state physics and optical communities, that the inverse of the Lyapunov exponent, γ^{-1}, and the localization length, l are always equal. While this is true for media with a continuous spatial distribution of the random dielectric constant, in the case of randomly layered samples, the situation, as we show in this paper, is much more complicated. In particular, the inverse of the Lyapunov exponent by itself, calculated, for example, in Ref. [20], does not provide comprehensive information about the transport properties of disordered media. Furthermore, it is unlikely that it can be measured directly, at least in the optical regime.

The first study of localization in metamaterials was presented in Ref. [21] where wave transmission through an alternating sequence of air layers and metamaterial layers of random thicknesses was studied. Localized modes within the gap were observed and delocalized modes were revealed despite the one-dimensional nature of the model. A more general model of alternating sequences of right- and left-handed layers with random parameters was studied in Ref. [22]. There, it has been shown that in mixed stacks (M-stacks) with fluctuating refractive indices, localization of low-frequency radiation was dramatically suppressed so that the localization length exceeded that for homogeneous stacks (H-stacks) composed solely of right- or left-handed slabs by many orders of magnitude, and scaling as $l \propto \lambda^6$ or even higher powers of wavelength (in what follows we refer to this result as the λ^6 anomaly), in contrast to the well-known dependence $l \propto \lambda^2$ observed in H-stacks [23]. As noted in Ref. [22], a possible physical explanation of this is the suppression of phase accumulation in M-stacks, related to the opposite signs of the phase and group velocities in left- and right-handed layers. Scaling laws of the transmission through a similar mixed multilayered structure were studied in [24]. There, it was shown that the spectrally averaged transmission in a frequency range around the fully transparent resonant mode decayed with the number of layers much more rapidly than in a homogeneous random slab. Localization in a disordered multilayered structure comprising alternating random layers of two different left-handed materials was considered in

Ref. [25], where it was shown that within the propagation gap, the localization length was shorter than the decay length in the underlying periodic structure, and the opposite of that observed in the corresponding random structure of right-handed layers.

In this paper, we study the wave transmission through disordered M- and H-stacks of a finite size composed of a weakly scattering right- and left-handed layers. In the framework of the weak scattering approximation (WSA), we have developed a unified theoretical description of the transmission and localization lengths over a wide wavelength range, allowing us to explain the pronounced difference in the transmission properties of M- and H-stacks at long wavelengths.

When both refractive index and layer thickness of the mixed stack are random, the transmission length in the long-wavelength part of the localized regime exhibits a quadratic power law dependence on wavelength with different constants of proportionality for mixed and homogeneous stacks. Such a difference has never been found in any disordered systems, and thus the M-stack is the first example of a disordered object in which the transmission and localization lengths differ. Both M- and H-stacks demonstrate a rather narrow crossover from the localized to ballistic regime. The H-stack in the near ballistic region, and the M-stack in the ballistic region are weakly scattering disordered stacks, while in the far ballistic region, the H-stack transmits radiation as an effectively uniform medium.

In M-stacks with only refractive index disorder, Anderson localization and transmission resonances are effectively suppressed and the crossover region between the localized and ballistic regimes is orders of magnitude greater. A more detailed study of the λ^6-anomaly shows that the genuine wavelength dependence of the transmission length is not described by any power law and rather is non-analytic in nature.

We also consider the effects of loss and show that absorption dominates the effects of disorder at very short and very long wavelengths. The crossover region is particularly sensitive to losses, so that even small absorption suppresses oscillations in the transmission length as a function of frequency.

All theoretical results, with the exception of the λ^6 anomaly, are confirmed by numerical simulation and are shown to be in excellent agreement.

In what follows, Sec. II presents a detailed description of our model. Section III is devoted to the analytical studies of the problem, while the results of numerical simulations and a discussion of these are presented in Sec. IV.

II. MODEL

A. Mixed and homogeneous stacks

We consider a one-dimensional alternating M-stack, as shown in Fig. 1. It comprises disordered mixed left- (L) and right- (R) handed layers, which alternate over its length of N layers, where N is an even number. The thicknesses of each layer are independent random values with the same mean value d. In what follows, all quantities with the dimension of length are measured in units of d. In these units, for the thicknesses of a layer we can write

$$d_j = 1 + \delta_j^{(d)},$$

where the fluctuations of the thickness, $\delta_j^{(d)}$, $j = 1, 2, \ldots$ are zero-mean independent random numbers.
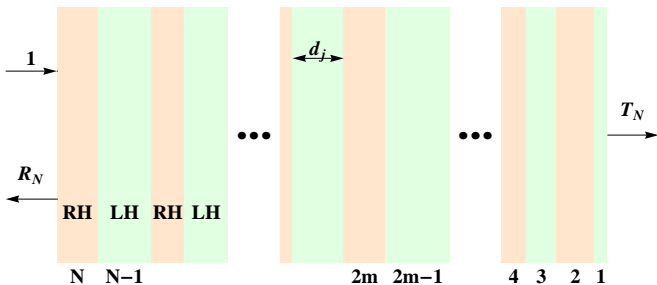

FIG. 1: Structure geometry

We take the magnetic permeability for right-handed media to be $\mu_j = 1$ and for metamaterials to be $\mu_j = -1$, while the dielectric permittivity is

$$\varepsilon_j = \pm (1 + \delta_j^{(\nu)} \pm i\sigma_j)^2,$$

where the upper and lower indices respectively correspond to normal (right-handed) and metamaterial (left-handed) layers. The refractive index of each layer is then

$$\nu_j = \pm(1 + \delta_j^{(\nu)}) + i\sigma_j,$$

where all $\delta_j^{(\nu)}$ and absorption coefficients of the slabs, $\sigma_j \geq 0$, are independent random variables. With this, the impedance of each layer relative to the background (free space) is

$$Z_j = \sqrt{\mu_j/\varepsilon_j} = 1/(1 + \delta_j^{(\nu)} \pm i\sigma_j),$$

with the same choice of the sign.

We begin with the general case when both types of disorder (in refractive index and in thickness) are present.

Two particular cases, each with only one type of disorder, are rather different. In the absence of absorption, the M-stack with only thickness disorder is completely transparent, a consequence of $Z_j \equiv 1$. However, the case of only refractive-index disorder is intriguing because, as is shown below, such mixed stacks manifest a dramatic suppression of Anderson localization in the long wave region [22].

Although localization in disordered H-stacks with right-handed layers has been studied by many authors [18, 23, 26–28], here we consider this problem in its most general form and show that the transmission properties of disordered H-stacks are qualitatively the same for stacks comprised of either solely left- or right-handed layers.

B. Transmission: localized and ballistic regimes

We introduce the transmission length l_N of a finite random configuration as

$$\frac{1}{l_N} = -\left\langle \frac{\ln |T_N|}{N} \right\rangle, \tag{1}$$

where T_N is the random transmission coefficient of a sample of the length N. As a consequence of the self-averaging of $\ln |T_N|/N$

$$\lim_{N \to \infty} \frac{\ln |T_N|}{N} = \lim_{N \to \infty} \frac{1}{l_N} = \frac{1}{l}. \tag{2}$$

This means that for a sufficiently long stack (in the localized regime) the transmission coefficient is exponentially small $|T_N| \sim \exp(-N/l)$.

In what follows, we consider stacks composed of layers with low dielectric contrasts, i.e, $|\delta^{\nu,d}| \ll 1$, so that the Fresnel reflection coefficients of each interface, and of each layer, are much smaller than 1. Here, a thin stack comprising a small number of layers is almost transparent. In this, the ballistic regime, the transmission length takes the form

$$\frac{1}{l_N} \approx \frac{\langle |R_N|^2 \rangle}{2N}, \tag{3}$$

with the average reflection coefficient given by [29]

$$\langle |R_N|^2 \rangle \approx \frac{2N}{b}, \quad N \ll b. \tag{4}$$

The length b in this equation is termed the *ballistic length*.

Thus, in studies of the transport of the classical waves in one-dimensional random systems, the following spatial scales arise in a natural way:

- l_N — the transmission length of a finite sample (1),

- l — the localization length (2), and

- b — ballistic length (4).

Note that in the case of absorbing stacks ($\sigma_j = \sigma > 0$), the right hand side of Eq. (1) defines the attenuation length, l_{att}, which incorporates the effects of both disorder and absorption.

In what follows, we show that contrary to commonly accepted belief, the quantities γ^{-1}, l, and b are not necessarily equal, and, under certain situations, can differ noticeably from each other.

In this paper, we study mainly the transmission length defined above by Eq. 1. This quantity is very sensitive to the size of the system and therefore is best suited to the description of the transmission properties in both localized and ballistic regimes. More precisely, the transmission length coincides either with the localization length or with the ballistic length, respectively in the cases of comparatively thick (localized regime) or comparatively thin (ballistic regime) stacks. That is,

$$
l_N \approx
\begin{cases}
l & N \gg l \\
b & N \ll b.
\end{cases}
$$

Another argument supporting our choice of the transmission length as the subject of investigation is that it can be found directly by standard transmission experiments, while measurements of the Lyapunov exponent call for a much more sophisticated arrangement.

III. ANALYTICAL STUDIES

A. Weak scattering approximation

The theoretical analysis involves the calculation of the transmission coefficient using a recursive procedure. Consider a stack which is a sequence of n layers enumerated by index j from $j = 1$ at the rear of the stack through to $j = n$ at the front. The total transmission (T_n) and reflection (R_n) amplitude coefficients of the stack satisfy the recurrence relations

$$
T_n = \frac{T_{n-1} t_n}{1 - R_{n-1} r_n}, \tag{5}
$$

$$
R_n = r_n + \frac{R_{n-1} t_n^2}{1 - R_{n-1} r_n} \tag{6}
$$

for $n = 2, \ldots, N$, in which both the input and output media are free space. In Eqs (5) and (6), the amplitude transmission (t_j) and the reflection (r_j) coefficients of a single layer are given by

$$
r_j = \frac{\rho_j(1 - e^{2i\beta_j})}{1 - \rho_j^2 e^{2i\beta_j}}, \tag{7}
$$

$$
t_j = \frac{(1 - \rho_j^2) e^{i\beta_j}}{1 - \rho_j^2 e^{2i\beta_j}}. \tag{8}
$$

Here, $\beta_j = k d_j \nu_j$, $k = 2\pi/\lambda$, and λ denotes the dimensionless free space wavelength. While the sign of the phase shift across each slab $\mathrm{Re}\,(\beta_j)$ varies according to the handedness of the material, the Fresnel interface coefficient ρ_j given by

$$
\rho_j = \frac{Z_j - 1}{Z_j + 1}, \tag{9}
$$

depends only on the relative impedance of the layer Z_j, a quantity whose real part is positive, irrespective of the handedness of the material.

Equations (5)-(9) are general and provide an *exact* description of the system and will be used later for direct numerical simulations of its transmission properties.

It was mentioned previously that we consider the special case of weak scattering for which the reflection from a single layer is small. i.e., $|r_j| \ll 1$. This occurs either for weak disorder, or for strong disorder provided that the wavelength is sufficiently long. The transmission length then follows from

$$
\ln |T_N|^2 = 2\mathrm{Re}\ln T_N \tag{10}
$$

and requires the following first order approximations derived from Eqs. (5) and (6):

$$
\ln T_n = \ln T_{1,n-1} + \ln t_n + R_{n-1} r_n, \tag{11}
$$

$$
R_n = r_n + R_{n-1} t_n^2. \tag{12}
$$

In deriving Eq. (12), we omit the first-order term $R_{n-1}^2 t_n^2 r_n$ since it contributes only to the second order of $\ln T_n$ already after the first iteration. Then, by summing up logarithmic terms (11), we obtain

$$
\ln T_N = \sum_{j=1}^{N} \ln t_j + \sum_{m=2}^{N} \sum_{j=m}^{N} r_{j-m+1} r_j \prod_{p=j-m+2}^{j-1} t_p^2. \tag{13}
$$

This equation enables us to derive a general expression for the transmission length $l_T(N)$ which is valid in all regimes (see the next Section). However, the ballistic length b, according to Eq. (4) (and the average reflection coefficient as well), is determined only by the total reflection amplitude R_N. In the ballistic regime, this amplitude coefficient, to the necessary accuracy, is given by

$$
R_N = \sum_{j=1}^{N} r_j. \tag{14}
$$

B. Mixed stack

1. General Approach

From here on, we assume that the random variables $\delta_j^{(\nu)}$ of left-handed or right-handed layers, $\delta_j^{(d)}$, and σ_j are identically distributed according to the corresponding probability density functions. This enables us to express all of the required quantities via the transmission and reflection amplitudes of a single right-handed or left-handed layer, $t_{r,l}$, $r_{r,l}$, and also to calculate easily all of the necessary ensemble averages.

The average of the first term in Eq. (13) can be written as

$$\left\langle \sum_{j=1}^{N} \ln t_j \right\rangle = \frac{N}{2}\langle \ln t_r \rangle + \frac{N}{2}\langle \ln t_l \rangle.$$

Next, we split the second term of Eq. (13) into two parts

$$\sum_{m=2}^{N}\sum_{j=m}^{N} r_{j-m+1} r_j \prod_{p=j-m+2}^{j-1} t_p^2 = N\mathcal{R}_1 + N\mathcal{R}_2,$$

where

$$\mathcal{R}_1 = \frac{1}{N}\sum_{m=1}^{N/2}\sum_{j=2m}^{N} r_{j-2m+1} r_j \prod_{p=j-2m+2}^{j-1} t_p^2,$$

$$\mathcal{R}_2 = \frac{1}{N}\sum_{m=1}^{N/2}\sum_{j=2m-1}^{N} r_{j-2m} r_j \prod_{p=j-2m+1}^{j-1} t_p^2.$$

comprising contributions to the depletion of the transmitted field due to two pass reflections respectively between slabs of different materials (i.e., of opposite handedness), and between slabs of the same material (i.e., of like handedness). Averaging these expressions, we obtain

$$\langle \mathcal{R}_1 \rangle = A_r A_l \left[\frac{1}{1-B^2} + \frac{(B^N-1)(1+B^2)}{N(1-B^2)^2} \right], \quad (15)$$

$$\langle \mathcal{R}_2 \rangle = \frac{A_r^2 B_l + A_r^2 B_l}{2N}\left[\frac{N}{1-B^2} + \frac{2(B^N-1)}{(1-B^2)^2} \right], \quad (16)$$

where

$$A_\tau = \langle r_\tau \rangle, \quad B_\tau = \langle t_\tau^2 \rangle, \quad \tau = l, r, \quad B^2 = B_l B_r. \quad (17)$$

The resulting transmission length is determined by the equation

$$-\frac{1}{l_N} = \frac{\langle \ln |t_r| \rangle + \langle \ln |t_l| \rangle}{2} + \mathrm{Re}\left(\langle \mathcal{R}_1 \rangle + \langle \mathcal{R}_2 \rangle \right). \quad (18)$$

In the lossless case ($\sigma = 0$), the first term on the right hand side of Eq. (18) corresponds to the so-called single-scattering approximation, which implies that multi-pass reflections are neglected so that the total transmission coefficient is approximated by the product of the single layer transmission coefficients, i.e.,

$$|T_N|^2 \rightarrow \prod_{j=1}^{N} |t_j|^2.$$

In the case of very long stacks (i.e., as the length $N \rightarrow \infty$), we can replace the arithmetic mean, $N^{-1}\sum_{j=1}^{N} \ln |t_j|$, by its ensemble average $\langle \ln |t| \rangle$. On the other hand, in this limit the reciprocal of the transmission length coincides with the localization length. Using the energy conservation law, $|r_j|^2 + |t_j|^2 = 1$, which applies in the absence of absorption, the inverse single-scattering localization length may be written as

$$\left(\frac{1}{l} \right)_{ss} = \frac{1}{2}\langle |r|^2 \rangle \quad (19)$$

and is proportional to the mean reflection coefficient of a single random layer [14, 34]. The corresponding modification of Eq. (18) then reads

$$\frac{1}{l_N} = \frac{\langle |r_r|^2 \rangle + \langle |r_l|^2 \rangle}{4} - \mathrm{Re}\left(\langle \mathcal{R}_1 \rangle + \langle \mathcal{R}_2 \rangle \right). \quad (20)$$

Here, the first term corresponds to the single-scattering approximation, while the two next terms take into account the interference of multiply scattered waves as well as the dependence of the transmission length on the stack size. Note that Eq. (20) is appropriate only for lossless structures. In the presence of absorption, Eq. (18) should be used instead.

2. Transmission length

From this point on, we assume that the statistical properties of the right-handed and left-handed layers are identical. As a consequence of this symmetry, the following relations hold for any real-valued function g in either the lossless or absorbing cases:

$$\langle g(t_r) \rangle = \langle g(t_l) \rangle^*, \quad \langle g(r_r) \rangle = \langle g(r_l) \rangle^*. \quad (21)$$

Therefore, A_r and B_r are the complex conjugates of A_l and B_l, and B^2 is real quantity, as are both averages $\langle \mathcal{R}_1 \rangle$ and $\langle \mathcal{R}_2 \rangle$.

Accordingly, as a consequence of the left-right symmetry 21, the transmission length of a M-stack depends only on the properties of a single right-handed layer and may be expressed in terms of three averaged characteristics: $\langle r \rangle$, $\langle \ln |t| \rangle$, and $\langle t^2 \rangle$ (in which we omit the subscript r).

With these observations, the transmission length of a finite length M-stack may be cast in the form:

$$\frac{1}{l_N} = \frac{1}{l} + \left(\frac{1}{b} - \frac{1}{l}\right) f(N, \bar{l}). \quad (22)$$

where

$$\frac{1}{l} = -\langle \ln |t| \rangle - \frac{|\langle r \rangle|^2 + \mathrm{Re}\left(\langle r \rangle^2 \langle t^2 \rangle^*\right)}{1 - |\langle t^2 \rangle|^2}. \quad (23)$$

and

$$\frac{1}{b} = \frac{1}{l} - \frac{2/\bar{l}}{1 - \exp(-2/\bar{l})} \times \\ \left(\frac{|\langle r \rangle|^2 + \mathrm{Re}\left(\langle r \rangle^2 \langle t^2 \rangle^*\right)}{1 - |\langle t^2 \rangle|^2} - \frac{|\langle r \rangle|^2}{2} \right) \quad (24)$$

are, as we will see below, the inverse localization and ballistic lengths. The function $f(N, \bar{l})$ is defined as

$$f(N, \bar{l}) = \frac{\bar{l}}{N}\left[1 - \exp\left(-\frac{N}{\bar{l}}\right)\right], \quad (25)$$

and introduces a new characteristic length termed the *crossover length*

$$\bar{l} = -\frac{1}{\ln |\langle t^2 \rangle|}, \quad (26)$$

which arises in the calculations in a natural way and, as will be demonstrated below, plays an important role in the theory of the transport and localization in one-dimensional random systems.

Equations (22)-(24) completely describe the transmission length of a mixed stack in the weak scattering approximation. Its value in the ballistic limit can be calculated directly from Eq. (4), with the average reflection coefficient, determined by Eq. (14), being

$$\left\langle |R_N|^2 \right\rangle = N\left(\left\langle |r|^2 \right\rangle - |\langle r \rangle|^2\right) + N^2 \left\langle \mathrm{Re}\, r \right\rangle^2. \quad (27)$$

Obviously, the characteristic lengths $l(\lambda)$, $b(\lambda)$, and $\bar{l}(\lambda)$ appearing in Eq. (22) are functions of wavelength. Using straightforward calculations, it may be shown that the first two always satisfy the inequality $l(\lambda) > b(\lambda)$, while, as we will see, the crossover length is the shortest of the three, i.e., $b(\lambda) > \bar{l}(\lambda)$ in the long wavelength region.

In the case of a fixed wavelength λ and a stack so short that $N \ll \bar{l}(\lambda)$, the expansion of the exponent in Eq. (25) yields $f \to 1$, in which case the transmission length approaches $b(\lambda)$. Correspondingly, for a sufficiently long stack, $N \gg \bar{l}(\lambda)$, $f \to 0$ and the transmission length assumes the value of $l(\lambda)$.

In summary,

$$l_N(\lambda) \approx \begin{cases} l(\lambda), & N \gg \bar{l}(\lambda), \\ b(\lambda), & N \ll \bar{l}(\lambda), \end{cases}$$

with the transition between the two ranges of N being determined by the crossover length.

While in the lossless case, the ballistic regime occurs when the stack is much shorter than the crossover length ($N \ll \bar{l}(\lambda)$), it is important to note that in the localization regime the opposite inequality is not sufficient and the necessary condition for localization is $N \gg l(\lambda)$. In what follows, we consider samples of an intermediate length, i.e., $\bar{l}(\lambda) \ll N \ll l(\lambda)$.

For an M-stack of the fixed size N, the parameter governing the transmission is the wavelength, and the conditions for the localized and ballistic regimes should be formulated in the wavelength domain. To do this, we introduce two characteristic wavelengths, $\lambda_1(N)$ and $\lambda_2(N)$, by the relations

$$N = l(\lambda_1(N)), \quad N = \bar{l}(\lambda_2(N)). \quad (28)$$

It can be shown that the long wavelength region, $\lambda \ll \lambda_1(N)$, corresponds to localization where the transmission length coincides with the localization length, while in the extremely long wavelength region, $\lambda \gg \lambda_2(N)$, the propagation is ballistic with the transmission length given by the ballistic length b. That is,

$$l_N(\lambda) \approx \begin{cases} l(\lambda), & \lambda \ll \lambda_1(N), \\ b(\lambda), & \lambda \gg \lambda_2(N). \end{cases} \quad (29)$$

When $\lambda_1(N) < \lambda_2(N)$, there exists an intermediate range of wavelengths, $\lambda_1(N) < \lambda < \lambda_2(N)$, which will be discussed below.

To better understand the physical meaning of the expressions (23) and (24) for the localization and ballistic lengths, we will consider ensembles of random configurations in which the fluctuations $\delta_j^{(\nu)}$ and $\delta_j^{(d)}$ are distributed uniformly over the intervals $[-Q_\nu, Q_\nu]$ and $[-Q_d, Q_d]$ respectively, with $\sigma_j = 0$. The average quantities that arise in Eqs. (23) and (24) are presented in Appendix. These formulae allow for calculations with an accuracy of order $O(Q_\nu^2)$ for arbitrary Q_d. For the sake of simplicity, we assume that the fluctuations of the refractive index and thickness are of the same order, i.e., $Q_\nu \sim Q_d$ so that the dimensionless parameter

$$\zeta = 2\frac{Q_d^2}{Q_\nu^2}$$

is of order of unity. We also neglect the contribution of terms of order higher than Q_d^2.

The short wavelength asymptotic of the localization length is then

$$l(\lambda) = \frac{12}{Q_\nu^2}. \qquad (30)$$

In the long wavelength limit, we obtain the following asymptotic forms for the corresponding single layer averages:

$$\langle r \rangle \approx \frac{ikQ_\nu^2}{6} - \frac{k^2Q_\nu^2}{2} - \frac{5ik^3Q_\nu^2}{9}, \qquad (31)$$

$$\langle \ln|t| \rangle \approx -\frac{k^2Q_\nu^2}{6}, \qquad (32)$$

$$\langle t^2 \rangle \approx 1 + 2ik + \frac{ikQ_\nu^2}{3} - \\ -2k^2 - \frac{5k^2Q_\nu^2}{3} + \frac{2k^2Q_d^2}{3}. \qquad (33)$$

Substitution of these expansions into Eq. (24) yields the long wavelength asymptotic of the ballistic length

$$b(\lambda) \approx \frac{3\lambda^2}{2\pi^2Q_\nu^2}. \qquad (34)$$

The same substitutions into Eq. (27) gives the average total reflection coefficient

$$\left\langle |R_N|^2 \right\rangle \approx \frac{Nk^2Q_\nu^2}{3}, \qquad (35)$$

which together with Eq. (4) again results in the value of the ballistic length given in Eq. (34).

Substituting the long wavelength expansions (31) - (33) into Eqs. (23) and (26), we derive the following asymptotic forms for the localization length

$$l(\lambda) \approx \frac{3\lambda^2}{2\pi^2Q_\nu^2} \frac{3+\zeta}{1+\zeta}, \qquad (36)$$

and the crossover length

$$\bar{l}(\lambda) \approx \frac{3\lambda^2}{2\pi^2Q_\nu^2} \frac{1}{4(3+\zeta)}. \qquad (37)$$

Using the well known transfer matrix approach [?] we can also calculate the long wavelength asymptotic of the M-stack Lyapunov exponent

$$\gamma = \frac{\pi^2\overline{d^2}}{2\lambda^2} \frac{\overline{\varepsilon^2} - \bar{\varepsilon}^2}{\bar{\varepsilon}}, \quad \varepsilon = (1+\nu)^2 \qquad (38)$$

which reduces to

$$\gamma = \frac{2\pi^2Q_\nu^2}{3\lambda^2} = \frac{1}{l} \frac{3+\zeta}{1+\zeta} > \frac{1}{l}. \qquad (39)$$

Thus, the disordered M-stack in the long wavelength region displays a unique example of a one-dimensional disordered system in which the localization length differs from reciprocal of the Lyapunov exponent.

The long wavelength asymptotics of the Lyapunov exponent $\gamma \propto \lambda^{-2}$ and corresponding asymptotics of the localization length, $l \propto \lambda^2$, Eq. (36), have a rather clear physical meaning. Indeed, in the limit as $\lambda \to \infty$, the propagating wave does not resolve the disorder since it is effectively averaged over distances of the order of the wavelength. This means that the localization is absent and the Lyapunov exponent $\gamma \propto l^{-1}$ vanishes. For large but finite wavelengths (i.e., small wavenumbers $k = 2\pi/\lambda$), the Lyapunov exponent is small and, assuming that its dependence on wavenumber is analytic, we can expand it in powers of k. This expansion commences with a term of order k^2 since the Lyapunov exponent is real and the wavenumber dependence enters field equations in the form (ik). Accordingly, in the long wavelength limit, $\gamma \propto k^2$ and so $l \propto \lambda^2$.

The main contribution to the ballistic length (34) is due to the final term in the right hand side of Eq. (24), which corresponds to the single-scattering approximation discussed at the end of the Sec. III B 1. While the ballistic length follows from the single scattering approximation, the calculation of the localization length (36) is more complex and requires that interference due to the multiple scattering of waves must be taken into account.

In the case under consideration ($Q_\nu \sim Q_d$ and $\zeta \sim 1$), the two characteristic wavelengths $\lambda_1(N)$ and $\lambda_2(N)$ (28) for an M-stack of a fixed length size N take the form

$$\lambda_1(N) = \pi Q_\nu \sqrt{\frac{2N}{3} \frac{1+\zeta}{3+\zeta}}, \qquad (40)$$

$$\lambda_2(N) = 2\pi Q_\nu \sqrt{2N\left(1+\frac{\zeta}{3}\right)} \qquad (41)$$

and are of the same order of magnitude. This means that the transmission length l_N coincides with the localization length (36) for $N \gg l(\lambda)$), and with the ballistic length (34) in the case when $N \ll \bar{l}(\lambda)$.

The crossover between the localized and ballistic regimes occurs for $\lambda_1(N) \lesssim \lambda \lesssim \lambda_2(N)$, with the two bounds being proportional to $Q_\nu\sqrt{N}$ and thus growing as $\sqrt{N}$. For long stacks, the transmission length in the crossover region can be described with high accuracy by the general equations (22) and (25), where the ballistic length $b(\lambda)$, the localization length $l(\lambda)$, and the crossover length $\bar{l}(\lambda)$ are replaced by their asymptotic forms (34) - (37). In the case of solely refractive index disorder ($Q_d \to 0$) when all thicknesses are set to unity, the ballistic length and the short wavelength asymptotic of the localization length coincide with the limiting values of their counterparts for an M-stack with both refractive index and thickness disorder (34) and (30). However, the corresponding limiting values of the long wavelength

localization length and crossover lengths have nothing to do with the genuine behaviour of the transmission length (see Sec. IV B 1). This means that the weak scattering approximation fails to describe the long wavelength asymptotics of the transmission length in both the localization and crossover regions. This is discussed in greater detail below.

Eqs. (15) - (18) (or Eqs. (22)- (26)) in the symmetric case completely determine the behaviour of the transmission length for a mixed stack composed of weakly scattering layers. Although $\bar{l}$ has been introduced as a crossover length, the entire region $N \gg \bar{l}$ does not necessarily support localization. Correspondingly, the ballistic regime may exist outside the region $N \ll \bar{l}$.

All of the results obtained under the symmetry assumption (21) are qualitatively valid in the general case. Indeed, the existence of the crossover (29) is related to the exponential dependence in Eq. (25) with a real and positive crossover length $\bar{l}$. When the assumption of symmetry no longer holds, this length takes a complex value. However, the quantity B in Eq. (16) satisfies (by its definition in Eq. (17)) the evident inequality $|B| < 1$. Therefore, the corresponding analogue of the function f (25) preserves all necessary limiting properties (see the next Sec. III B 3).

3. Homogeneous stacks

In this Section, we consider an H-stack composed entirely of normal material layers noting that the behaviour of an H-stack of metamaterial (left-handed) layers alone is exactly the same, a result which may be obtained directly from Eq. (18) by replacing each l by r, after which any reference to the index r may be omitted. The transmission length of an H-stack is then

$$\frac{1}{l_N} = \frac{1}{l} + \frac{1}{N} \operatorname{Re}\left[\langle r \rangle^2 \frac{1 - \langle t^2 \rangle^N}{(1 - \langle t^2 \rangle)^2}\right], \qquad (42)$$

where the inverse localization length l is

$$\frac{1}{l} = -\langle \ln|t| \rangle - \operatorname{Re}\frac{\langle r \rangle^2}{1 - \langle t^2 \rangle}. \qquad (43)$$

Now we consider a H-stack composed of weakly scattering layers. To simplify the discussion, we consider only refractive index disorder (i.e., $Q_d = 0$). In this case, the asymptotic behavior of the localization length in the short and long wavelength limits are

$$l(\lambda) = \begin{cases} \dfrac{12}{Q_\nu^2}, & \lambda \to 0, \\[2ex] \dfrac{3\lambda^2}{2\pi^2 Q_\nu^2}, & \lambda \to \infty. \end{cases} \qquad (44)$$

The main contribution to the localization length is related to the first term in Eq. (43). Thus, the localization length of the H-stack in the long wavelength region is described completely by the single scattering approximation and coincides with the ballistic length (34) of the M-stack.

Using the transfer matrix approach we can also calculate the long wavelength asymptotic of the Lyapunov exponent for a H-stack . It is described by the the same equation (38) as the asymptotic for the M-stack, thus coinciding with the asymptotic of the reciprocal Lyapunov exponent. In recent work [20], this coincidence was established analytically in a wider spectral region. However, the numerical calculations intended to confirm this result are rather unconvincing. Indeed, the numerically obtained plots demonstrate strong fluctuations (of the same order as the mean value) of the calculated quantity, while the genuine Lyapunov exponent is non-random and should be smooth without any additional ensemble averaging mentioned by the authors.

If we present $\langle t^2 \rangle^N$ in the second term of Eq. (42) in the form $\exp\left(N \ln\langle t^2 \rangle\right)$ we see that the crossover length of the H-stack is

$$\bar{l} = \left| \ln\langle t^2 \rangle \right|^{-1},$$

with its long wavelength asymptotic, according to Eq. (33), being

$$\bar{l}(\lambda) = \frac{\lambda}{4\pi}. \qquad (45)$$

Here, the crossover length is proportional to the wavelength, in stark contradistinction to the situation for M-stacks, in which the crossover length is proportional to λ^2.

To consider this further, we define the characteristic wavelengths $\lambda_1(N)$ and $\lambda_2(N)$ by the expressions (28). For a H-stack, these lengths are

$$\begin{aligned} \lambda_1(N) &= \pi Q_\nu \sqrt{\frac{2N}{3}}, \\ \lambda_2(N) &= 4\pi N. \end{aligned} \qquad (46)$$

Evidently, the second characteristic wavelength is always much larger than the first $\lambda_2(N) \gg \lambda_1(N)$. As a consequence, the long wavelength region, where the ballistic regime is realized, can be divided into two subregions. The near subregion (moderately long wavelengths) is bounded by the characteristic wavelengths

$$\lambda_1(N) \lesssim \lambda \lesssim \lambda_2(N).$$

The main contribution to the ballistic length in the near ballistic region, b_n, is due to the first term in Eq. (43). Thus the ballistic length $b_n(\lambda)$ has the same wavelength dependence as the localization length $l(\lambda)$ (44)

$$b_n(\lambda) = \frac{3\lambda^2}{2\pi^2 Q_\nu^2},$$

and is well described by the single scattering approximation (19). For an H-stack , the transition from the localized to the ballistic regime at $\lambda \sim \lambda_1(N)$ is not accompanied by any change of the wavelength dependence of the transmission length. This change can occur at much longer wavelengths $\lambda \sim \lambda_2(N)$ in the far long wavelength subregion.

To derive the ballistic length b_f in the far long wavelength region, we may proceed in a similar manner to that outlined in the case of a M-stack and expand the exponent $\langle t^2 \rangle^N = \exp\left(N \ln\langle t^2 \rangle\right)$ in Eq. (42). However, because $< t^2 >$ in this expression is complex, the situation is more complicated than was the case for the M-stack. In particular, two first terms of the expansion do not contribute to the ballistic length. Taking account of the second order leads to the following expression for the ballistic length, $b_f(\lambda)$, in the far long wavelength region

$$\frac{1}{b_f(\lambda)} = \frac{2\pi^2 Q_\nu^2}{3\lambda^2} + \frac{N\pi^2 Q_\nu^4}{18\lambda^2}. \qquad (47)$$

In the case of a relatively short H-stack $NQ_\nu^2/12 \ll 1$, the contribution of the first term in the right hand side of this equation dominates, and hence the transition from the near to the far subregions is not accompanied by any change in the analytical dependence on the wavelength. The ballistic length is thus described by the same wavelength dependence over the entire ballistic region

$$b(\lambda) = \frac{3\lambda^2}{2\pi^2 Q_\nu^2}, \quad \lambda_1(N) \ll \lambda. \qquad (48)$$

For sufficiently long H-stacks $NQ_\nu^2/12 \gg 1$, in the far long wavelength region, the second term is dominant and so

$$b_f(\lambda) = \frac{18\lambda^2}{N\pi^2 Q_\nu^4}. \qquad (49)$$

Thus the wavelength dependence of the ballistic length of a sufficiently long H-stack is

$$b(\lambda) = \begin{cases} \dfrac{3\lambda^2}{2\pi^2 Q_\nu^2}, & \lambda_1(N) \lesssim \lambda \lesssim \lambda_2(N), \\[2mm] \dfrac{18\lambda^2}{N\pi^2 Q_\nu^4}, & \lambda_2(N) \lesssim \lambda. \end{cases} \qquad (50)$$

The same result for the ballistic length also follows from Eq. (4) with Eq. (14) in the case of a homogeneous stack yielding

$$\left\langle |R_N|^2 \right\rangle = N\left(\left\langle |r|^2 \right\rangle - |\langle r \rangle|^2\right) + N^2 |\langle r \rangle|^2. \qquad (51)$$

In the long wave limit this leads to

$$\left\langle |R_N|^2 \right\rangle = \frac{Nk^2 Q_\nu^2}{3} + \frac{N^2 k^2 Q_\nu^4}{36}, \quad \lambda_1(N) \ll \lambda, \qquad (52)$$

which together with Eq. (4) is equivalent to the result in Eqs. (48) and (50), applicable to short and long stack respectively.

The far long wavelength ballistic asymptotic (49) has a simple physical interpretation. Indeed, in this subregion, the wavelength essentially exceeds the stack size and so we may consider the stack as a single weakly scattering uniform layer with an effective refractive index n_{eff}. In this case, the ballistic length of the stack according to Eq. (4) is

$$b_f = \frac{2N}{|R_{\text{eff}}|^2}, \qquad (53)$$

where

$$R_{\text{eff}} = \frac{ikN}{2}\left(\nu_{\text{eff}}^2 - 1\right) \qquad (54)$$

is the long wavelength form of the reflection amplitude for a uniform stack of the length N and constant refractive index ν_{eff}.

To calculate the effective refractive index we use Eq. (14). Neglecting small fluctuations of the layer thickness, the single layer reflection amplitude in the long wavelength limit reads

$$r_j = \frac{ik}{2}\left(\nu_j^2 - 1\right). \qquad (55)$$

The total reflection amplitude for a stack of the length N is

$$R_N = \frac{ik}{2}\sum_{j=1}^{N}\left(\nu_j^2 - 1\right) = \frac{ikN}{2}\left(\frac{1}{N}\sum_{j=1}^{N}\nu_j^2 - 1\right), \qquad (56)$$

corresponding to the effective refractive index determined by the expression

$$\nu_{\text{eff}}^2 = \frac{1}{N}\sum_{j=1}^{N}\nu_j^2. \qquad (57)$$

For sufficiently long stacks, the right hand side of Eq. (58) can be replaced by the ensemble average $\langle \nu_j^2 \rangle$ and hence

$$\nu_{\text{eff}}^2 = \langle \nu_j^2 \rangle \approx 1 + \frac{Q_\nu^2}{3}. \tag{58}$$

This together with Eqs. (53), (54), and (58) leads immediately to the far long wavelength ballistic length (49).

We emphasize that because of the effective uniformity of the H-stack in the far ballistic region, the transmission length on a single realization is non-random (like the localization length), while in the near ballistic region it fluctuates strongly, as it does over the whole ballistic region for M-stacks.

To characterize the entire crossover region between the two ballistic regimes (50) in greater detail we return to the general formula (42), in which we represent $\langle t^2 \rangle^N$ as $e^{N \ln \langle t^2 \rangle}$. Then, in accordance with Eq.33, we can write

$$\langle t^2 \rangle^N \approx \exp\{N(2ik - k^2 Q_\nu^2) \approx (1 - Nk^2 Q_\nu^2)\exp 2ikN. \tag{59}$$

As a consequence, instead of the result in Eq. (47), we obtain

$$\frac{1}{b_n(\lambda)} = \frac{2\pi^2 Q_\nu^2}{3\lambda^2} + \frac{Q_\nu^4}{72N} \sin^2 \frac{2\pi N}{\lambda}. \tag{60}$$

We note that, strictly speaking, the expansion (59) is valid inside the interval $\sqrt{6}\lambda_1(N) \ll \lambda \ll \lambda_2(N)$.

The second term in Eq. (60) represents standard oscillations of the reflection coefficient of a uniform slab of finite size. In the far long wavelength limit $\lambda \gg \lambda_2$, this equation coincides with (47). Thus, Eq. (60) describes the ballistic length over practically the whole ballistic region $\lambda \gg \lambda_1(N)$. Moreover, taking into account that the long wavelength asymptotic of the localization length coincides with that of the near long wavelength ballistic length, we see that the right hand side of Eq. (60) serves as an excellent interpolation formula for the reciprocal of the transmission length $1/l_N(\lambda)$ of a sufficiently long stack ($NQ_\nu^2/12 \gg 1$) over the entire long wavelength region $\lambda \gg 1$.

C. Comparison of the transmission length behaviour in M- and H- stacks

Away from the transition regions, the transmission length can exhibit three types of long wavelength asymptotics described by the right hand sides of Eqs. (34), (36), and (49). The first (34) corresponds to the single scattering approximation where the inverse transmission length is proportional to the average reflection coefficient of a single random layer. It characterizes both the localization and ballistic lengths. The second asymptotic form (36) takes into account the interference of multiple scattered waves and describes the localization length. The third asymptotic (49) corresponds to transmission

through a uniform slab with an effective dielectric constant given by Eq. (58) and is relevant only in the ballistic regime.

In the case of a M-stack, the first two expressions (34) and (36) characterize the ballistic and localized regimes respectively, while the third asymptotic is never realized in M-stacks. In relatively short H-stacks (48), the long wavelength behaviour of the transmission length is described by the same dependence (34) in both the localized and ballistic regimes. Finally, in the case of long H-stacks (49), the transmission length follows from Eq. (34) in the localized and near ballistic regimes, while in the far ballistic region it is described by the right hand side of Eq. (49).

These results predict the existence of a different wavelength dependence of the transmission length in different wavelength ranges. For M-stacks, the crossover between them occurs at the wavelength $\lambda_1(N)$ (40) where the size of the stack is comparable with the localization length $l(\lambda_1(N)) \approx N$. For long H-stacks, the crossover occurs when the wavelength becomes comparable to the stack size $\lambda \approx N$. Short H-stacks exhibit the same wavelength dependence of the transmission length in all long wavelength regions, i.e., in both localized and ballistic regimes.

IV. NUMERICAL RESULTS

The results of the numerical simulations presented below correspond to uniform distributions of the fluctuations $\delta^{(d)}$, $\delta^{(\nu)}$, with widths of Q_ν and Q_d, respectively, and with a constant value of the absorption σ.

Results are presented for (a) direct simulations based on the exact recurrence relations (5) and (6); (b) weak scattering analysis for the transmission length based on Eqs. (22) and (42); and (c) for short (30) and long wavelength [(34), (36), and (49)] asymptotics. For the mean reflectivity, we used the asymptotics (35), (60).

In all cases, unless otherwise is mentioned, the ensemble averaging is taken over $N_r = 10^4$ realizations. The results up to Sec. IV C are for lossless stacks ($\sigma = 0$) only.

A. Refractive-index and thickness disorder

We first consider stacks having refractive index and thickness disorder, with $Q_\nu = 0.25$ and $Q_d = 0.2$. Shown in Fig. 2 are transmission spectra for a M-stack of $N = 10^5$ layers and a H-stack of length $N = 10^3$. There are two major differences between the results for these two types of samples: first, in the localized regime ($N \gg l_N$), the transmission length of the M-stack exceeds or coincides with that of the H-stack; second, in the long-wavelength region, the plot of the transmission length of the M-stack manifests a pronounced bend or kink in the interval $\lambda \in [10^2, 10^3]$, while there is no such feature in

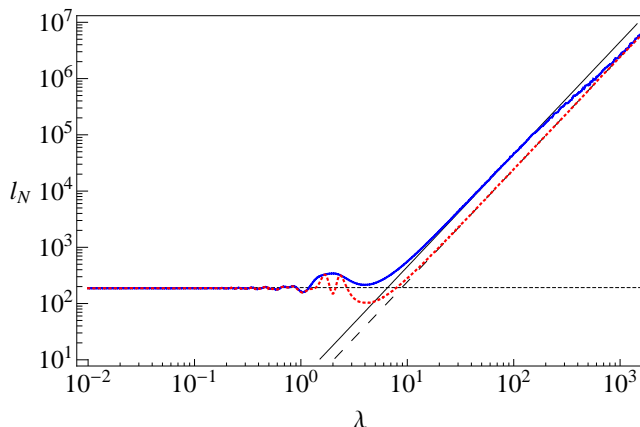the H-stack results. These two types of behaviour are discussed in more detail below.

FIG. 2: Transmission length l_N vs λ for M-stack (thick solid line) and H-stack (thick dashed line). Asymptotics of the localization length l (thin straight lines), the short wavelength asymptotic (thin dotted line, (30), and the long wavelength asymptotics—thin solid line for the M-stack (36) and a thin dashed line for the H-stack (44).

1. Mixed stacks

The weak scattering approximation (WSA) of Eq. (18) is an excellent method by which to calculate the transmission length for M-stacks. This is seen in Fig.2 where the curves obtained by numerical simulations and by the WSA are indistinguishable (solid line). The characteristic wavelengths (40) of this mixed stack are $\lambda_1 \approx 148$ and $\lambda_2 \approx 839$. Therefore, the transmission length describes the localization properties of a random sample in the region $\lambda \lesssim 148$, whereas longer wavelengths, $\lambda \gtrsim 839$, correspond to the ballistic regime. The crossover from the localized to the ballistic regime demonstrates the kink-type behaviour that occurs within the region $\lambda_1 \lesssim \lambda \lesssim \lambda_2$. The short and long wavelength behaviour of the transmission length is also in excellent agreement with the calculated asymptotics in both regimes.

To analyze the long wavelength region ($\lambda \gtrsim 10$) more carefully, we plot in Fig. 3 the transmission lengths of M-stacks of three different sizes, $N = 10^3$, 10^5, and 10^7. In all cases, there is excellent agreement between the simulations and the WSA predictions. The characteristic wavelengths for $N = 10^3$ are $\lambda_1 = 14.8$ and $\lambda_2 = 83.9$, while for $N = 10^7$ they are $\lambda_1 = 1480$ and $\lambda_2 = 8390$, and we see that the observed crossover regions are bounded exactly by these characteristic wavelengths in all three cases.

To confirm the ballistic nature of the transmission in the region $\lambda > \lambda_2$, we plot in Fig. 4(a) the logarithm of the mean value of the reflectance for the same three
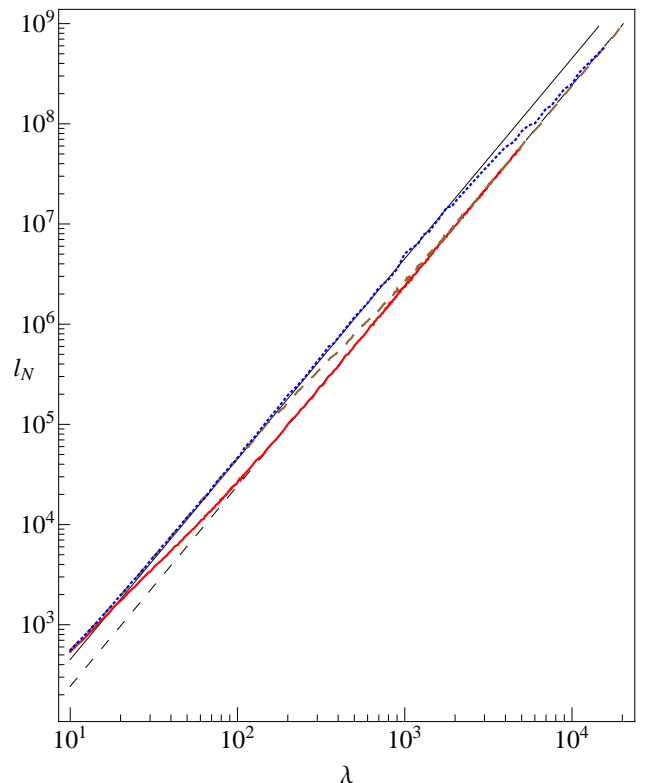

FIG. 3: Transmission length l_N vs λ for a M-stack of $N = 10^3$ (thick solid line), 10^5 (thick dashed line) and 10^7 (thick dotted line) layers showing both numerical simulations and the WSA theory. The long wave asymptotics for the localization length (36) and the ballistic length (34) are shown respectively in the thin solid and dashed lines respectively.

stack sizes as a function of the logarithm of the wavelength. In all cases, the plots exhibit a linear dependence $\ln\langle |R_N|^2 \rangle = \text{const} + 2\ln\lambda$ in the ballistic regime which is bounded from below by the crossover wavelength λ_2. The straight lines are calculated from Eq. (35) and confirm that the reflection coefficient in the mixed stack is proportional to the stack length. Within the localized region $\lambda \lesssim \lambda_1$, the reflection coefficient is close to unity in all three cases.

The behaviour of the transmission length is illustrated by the phase diagram in the (λ, N) plane shown in Fig. 4(b). The two slanted lines $N = l(\lambda)$ and $N = \bar{l}(\lambda)$ separate the plane into three parts corresponding to the localization (I), the crossover region (II) and the ballistic region (III). Crossing points of these lines with the horizontal lines $N = 10^3$, $N = 10^5$, and $N = 10^7$ define the characteristic wavelengths λ_1 and λ_2 for the three stack sizes considered here. It is easy to see that these wavelengths, determined with the aid of the phase diagram, perfectly bound the crossover regions in both Fig. 3 and Fig. 4(a).
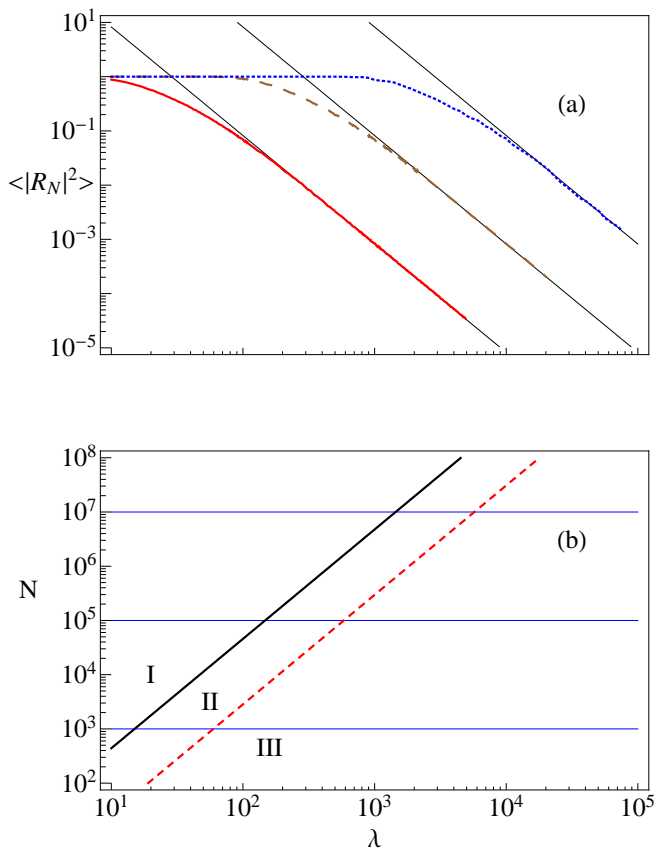
FIG. 4: (a) Average reflectance for M-stacks of length $N = 10^3$ (solid line), 10^5 (dashed line) and 10^7 (dotted line) layers (numerical simulation and WSA). Long wave asymptotic for the average reflectance for the same stacks (thin solid lines). (b) Phase diagram of M-stacks. The thick solid line corresponds to a stack size equal to the localization length. The dashed line corresponds to a stack size equal to the crossover length. The localized, crossover and ballistic regimes occur in regions I, II, and III respectively.

2. Homogeneous stacks

The absence of any kink in the H-stack transmission length spectrum in Fig. 2 follows from Sec. III B 3 in which it was shown that the crossover to the far ballistic regime occurs at the wavelength $\lambda_2(N)$ (45). For $N = 10^3$, this is of the order of 10^4 and so the kink does not appear.

In order to study the crossover, we plot in Fig. 5 the transmission lengths of H-stacks with $N = 10^3$ and 10^4 over the wavelength range extended up to $\lambda \sim 10^6$. As for the M-stack, the simulation results for H-stacks cannot be distinguished from those of the WSA (42). The transition from the localized to the near ballistic regime occurs without any change of the analytical dependence of transmission length, in complete agreement with the results of Sec. III B 3. The crossover from the near to the far ballistic regime is accompanied by a change in
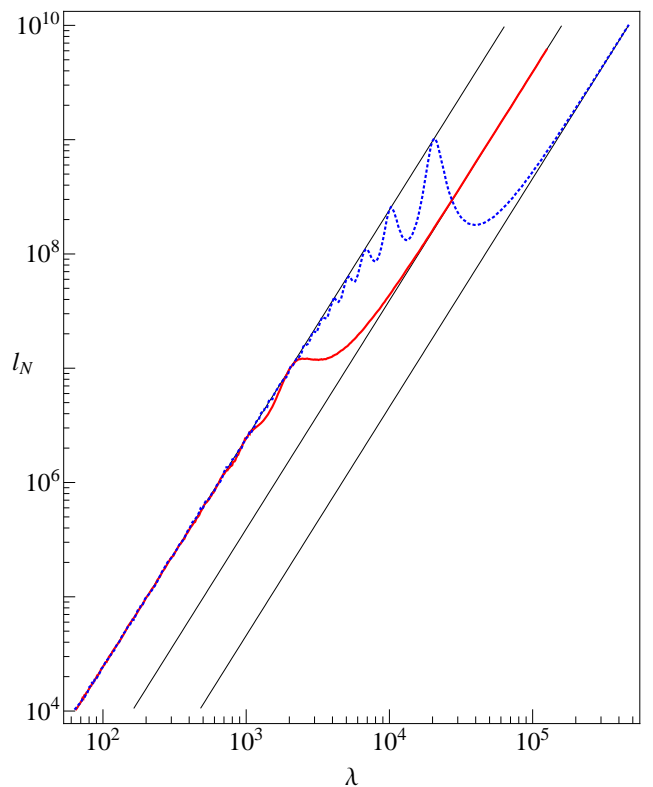

FIG. 5: Transmission length l_N vs λ for H-stacks of $N = 10^3$ (solid line), and 10^4 (dotted line) layers (numerical simulation and WSA). Long wave asymptotics for the ballistic length in the near and far ballistic regions are plotted in thin solid lines.

the analytical dependence, that occurs at $\lambda = \lambda_2(N)$, which for these stacks is of the order of 10^4 and 10^5 respectively. The crossover is accompanied by prominent oscillations described by Eq. (60). Finally, we note that the vertical displacement between the moderately long and extremely long wavelength ballistic asymptotes does not depend on wavelength, but grows with the size of the stack, according to the law

$$\ln \frac{b_n}{b_f} = \ln \frac{NQ_\nu^2}{12}, \qquad (61)$$

which stems from Eq. (50).

To study the ballistic transmission regime in the region $\lambda > \lambda_1$ more closely, we plot in the upper panel of Fig. 6(a) in a logarithmic scale the mean value of the reflection coefficient for the same two stack sizes. That part of each plot which presents the ballistic propagation comprises two linear asymptotes of the form $\ln\langle|R_N|^2\rangle = \text{const} + 2\ln\lambda$, corresponding to different values of the constant, one applicable in the near ballistic region $\lambda_1(N) \lesssim \lambda \lesssim \lambda_2(N)$ and the other in the far ballistic region $\lambda_2(N) \lesssim \lambda$. The difference between the values of these two constants corresponds precisely with the right hand side of Eq. (61), with the far long wavelength asymptotic given by the second term in Eq. (60).

Within the localized regime $\lambda \lesssim \lambda_1(N)$, the reflectance is almost unity in all three cases.
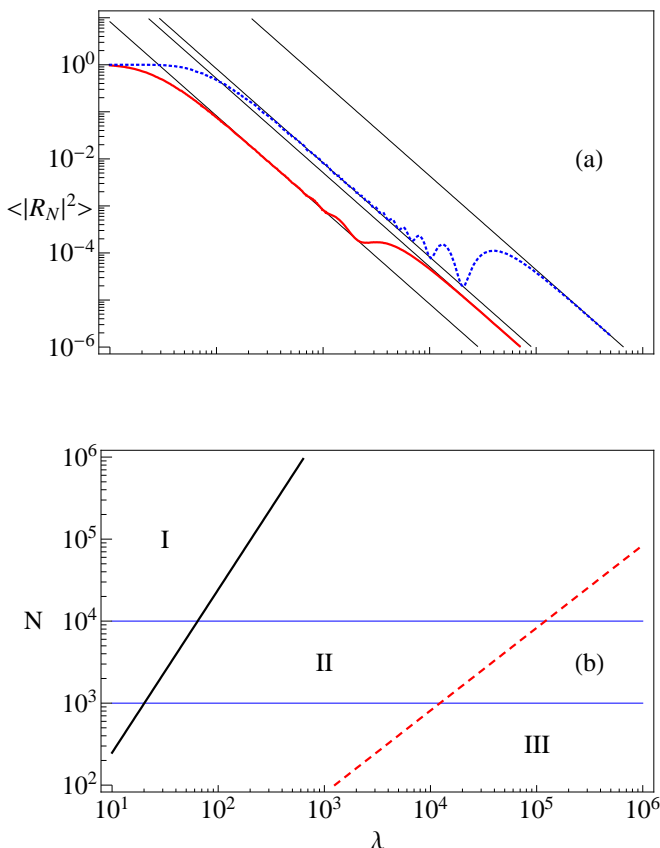

FIG. 6: (a) Average reflectance from H-stacks of $N = 10^3$ (solid line), and 10^4 (dotted line) layers (numerical simulation and WSA). Long wave asymptotics of the ballistic length in the near and far ballistic regions are plotted by thin solid lines. (b) Phase diagram of H-stack. The thick solid line corresponds to where the stack size equals the localization length. The dashed line corresponds to where the stack size equals the crossover length, while the localized, near ballistic and far ballistic regimes correspond to regions (I), (II), and (III) respectively.

By analogy with M-stacks, the behaviour of the transmission length in the (λ, N) plane is illustrated by the phase diagram displayed in the lower panel of Fig. 6. Two slanted lines $N = l(\lambda)$ and $N = \bar{l}(\lambda)$ divide the plane into three parts corresponding to the localization regime (I), the crossover regime (II) and the ballistic regime (III). The wavelength, at which these slanted lines intersect the horizontal lines corresponding to the stack lengths, $N = 10^3$, and $N = 10^4$ defines the characteristic wavelengths (46) for each stack size. From Fig. 6(b), it follows that the separation between them grows with increasing size in accordance with Eq. (61). It is easy to see that the wavelengths $\lambda_{1,2}$ determined from the phase diagram perfectly bound the near ballistic region in both Fig. 5 and Fig. 6(a).

As mentioned in Section III B 3, the transmission length for any single realization in the far ballistic region becomes non random. To confirm this observation we shown in Fig. 7 that although $\tilde{l}_N$ exhibits fluctuations in the near ballistic region, it is a fairly smooth function of wavelength in the far ballistic regime.
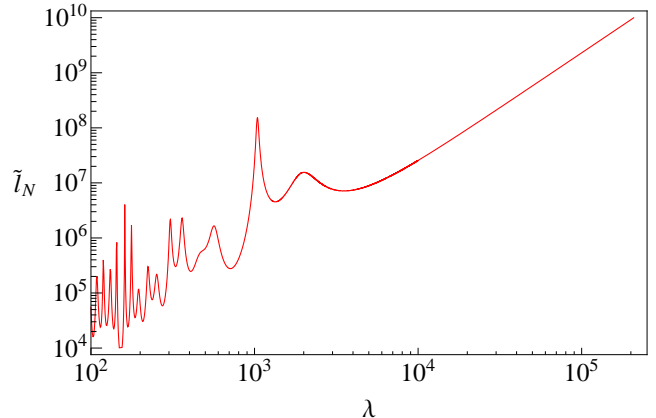

FIG. 7: Transmission length for a single realization $\tilde{l}_N$ of a H-stack of length $N = 10^3$ and with $Q_\nu = 0.25$, $Q_d = 0$

Until now, we have dealt only with the transmission length. However, some useful information is contained in the transmission length for a single realization defined by the equation

$$\frac{1}{\tilde{l}_N} = -\frac{\ln |T_N|}{N}. \tag{62}$$

Although this definition does not contain ensemble averaging, in the following two cases the transmission length determined from one realization becomes non-random in the localized regime (for both M- and H-stacks) because of self-averaging nature of $1/l_N$, and in the far ballistic region, for H-stacks only, because of the effective uniformity of the stack in this region.

In summary, we note that the results of Sec. IV A show excellent agreement between the numerical simulations and the analytical predictions of the weak scattering approximation of Sec. III. Moreover, even for the case of an H-stack of length $N = 10^3$ and strong disorder, $Q_\nu = 0.9$ and $Q_d = 0.2$, the results of direct simulation and those of the WSA analysis coincide completely in the long wavelength region and differ by only a few percent in the short wave region where the scattering is certainly not weak. This is because the perturbation approach based on Eqs. (11), (12) is related not to the calculated quantities but to the equations they satisfy.

B. Refractive-index disorder

1. Suppression of localization

Here, we present the results for stacks with only refractive index disorder (RID) with $Q_\nu = 0.25$. For H-stacks, the transmission length demonstrates qualitatively and quantitatively the same behaviour as was observed in the presence of both refractive index and thickness disorder. Corresponding formulae for the transmission, localization, and ballistic lengths can be obtained from the general case by taking the limit as $Q_d \to 0$.

In the case of M-stacks, however, the situation changes markedly. While in the short wavelength region and in the ballistic regime the numerical results are still in a excellent agreement with the predictions of the weak scattering approximation, the WSA fails in the long wavelength part of the localization regime. This discrepancy manifests itself also for short stacks, in which the localization regime in the long wave region is absent. In Fig. 8 we present the transmission length spectrum for a M-stack of $N = 10^3$ layers, showing that, for $\lambda \approx 5$, the numerical results for the transmission lengths of M-stacks differ by an order of magnitude from those predicted by the WSA analysis, and also those observed for the corresponding H-stacks.
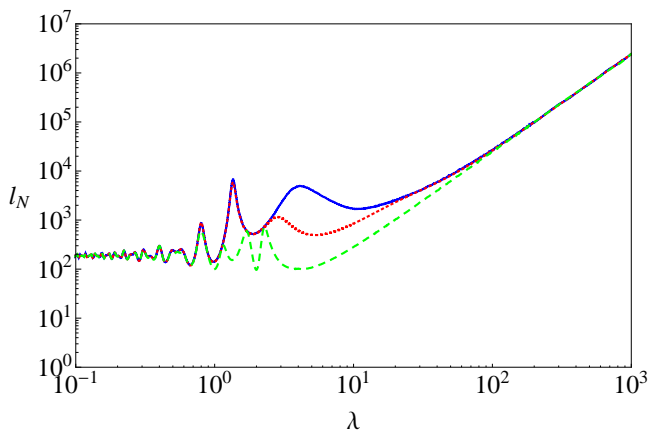

FIG. 8: Transmission length l_N vs wavelength λ for stacks of $N = 10^3$ layers. M-stack: numerical simulation (solid line), WSA (dotted line). H-stack: numerical simulation and WSA (both dashed lines).

For longer stacks, the differences in the transmission length spectra exhibited by M-stacks and H-stacks becomes much more pronounced. In Fig. 9, we plot transmission length spectra for different values of the M-stack length with $N = 10^7$ (using 10^3 realizations), 10^9 (using 10^3 realizations) and 10^{12} layers (using only a single realization), with the dashed-dotted straight line in Fig. 9 showing the long wavelength ballistic asymptote (34). In the moderately long wavelength region corresponding to the localization regime, the transmission length $l_N \ll N$

coincides with the localization length l. It exceeds the H-stack localization length by a few orders of magnitude and is characterized by a completely different wavelength dependence. This substantial suppression of localization was revealed in our earlier paper [22] where the localization length l_N was reported to be proportional to λ^6, in contrast to the classical λ^2 dependence (36) that is observed for H-stacks, and which is also valid for M-stacks with both refractive index and thickness disorder. The reason for this difference is the lack of phase accumulation caused by the phase cancelation in alternating layers of equal thicknesses.
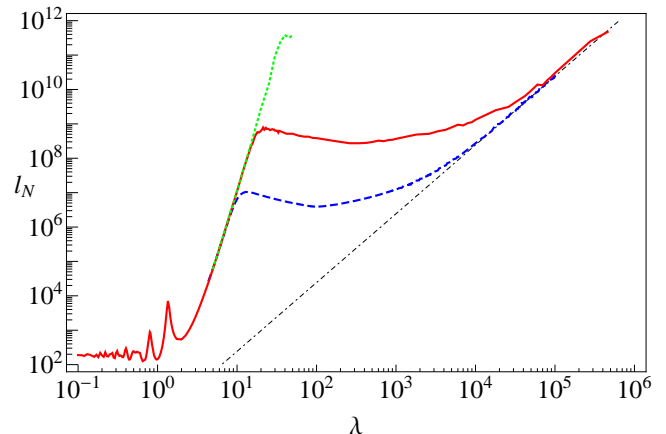

FIG. 9: Transmission length l_N vs wavelength λ for an M-stack with $Q_\nu = 0.25$, $Q_d = 0$ and $N = 10^7$ (dashed line), $N = 10^9$ (solid line), and $N = 10^{12}$ (dotted line) layers.

To study this behaviour in more detail, we generate a least squares fit $l_N = A\lambda^p$ to the transmission length data. Respectively, for $N = 10^7$, 10^9, and 10^{12} layers, the best fits are $l_N = 4\lambda^{6.25}$, $l_N = 0.43\lambda^{7.38}$ and $l_N = 0.01\lambda^{8.78}$, indicating that the asymptotic form for the localization length differs from a pure power law, and perhaps is described by a non-analytic dependence.

In the crossover part of the long-wave region where $l_N \approx N$, the transmission length of M-stacks also differs essentially from that for H-stacks. Moreover, the width of the crossover region on the l_N−axis remains of the same order of magnitude, although on the λ−axis it grows for $N = 10^9$ to four orders of magnitude, being much wider for longer stacks. In the long wavelength region corresponding to the ballistic regime, the transmission length of the RID M-stack coincides with that of RID H-stack.

As was mentioned above, the transmission length $\widetilde{l}(N)$ for a single realization approaches its non-random limit l as $N \to \infty$. This means that in the localization region, the dependence $\widetilde{l}(N)$ should be rather smooth because of self-averaging, while outside this region fluctuations must occur. To check this, we plot in Fig.10 $\widetilde{l}(N)$ and the transmission length l_N as functions of wavelength λ for a RID M-stack of $N = 10^4$ layers. We note that in the localized part of the spectrum, $\lambda < 5$, the ensemble
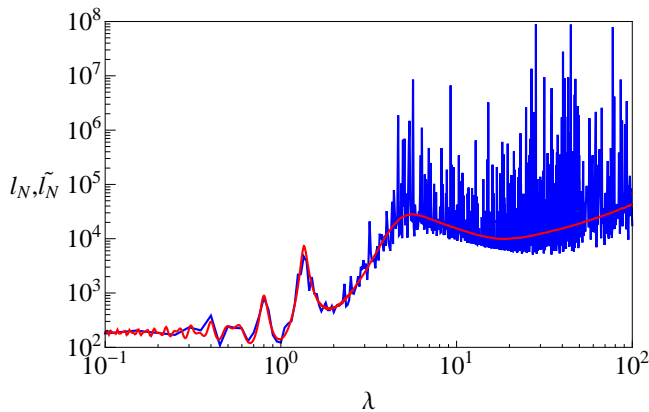
FIG. 10: Transmission length l_N vs λ for an M-stack with $Q_\nu = 0.25$, $Q_d = 0$ and $N = 10^4$ layers (solid line) and the transmission length for a realization $\tilde{l}_N$ for the same values Q_ν, Q_d (dashed line). Each wavelength corresponds to a different realization of the refractive index.

averaged and single realization curves are close, revealing that the self-averaging property of $\tilde{l}(N)$ holds for mixed media. Within the crossover region, however, the dependence of $\tilde{l}$ on λ demonstrates prominent fluctuations.

2. Transmission resonances

An important signature of the localization regime is the presence of transmission resonances (see, for example, Refs. [30–32]), which appears in sufficiently long, open systems and which present a "fingerprint" of a given realization of disorder. These resonances are responsible for the difference between two quantities that characterize the transmission, namely $\langle \ln |T|^2 \rangle$ and $\ln \langle |T|^2 \rangle$. The former reflects the properties of a typical realization, while the main contribution to the latter is generated by a small number of almost transparent realizations associated with the transmission resonances.

The natural characteristic of the transmission resonances is the ratio of the two quantities mentioned above:

$$ s = \frac{\langle \ln |T|^2 \rangle}{\ln \langle |T|^2 \rangle}. $$

In the absence of resonances, this value is close to unity, while in the localization regime $s > 1$. In particular, in the high-energy part of the spectrum of a disordered system with Gaussian white-noise potential, this ratio takes the value 4 [14].

In Fig. 11, we plot the ratio $s(\lambda)$ as a function of the wavelength for RID M- and H-stacks and for the corresponding stacks with thickness disorder. In all cases, the stack length is $N = 10^3$ and it is evident that for the RID M-stack $s(\lambda) \approx 1$, i.e. the stack length is too short for the localization regime to be realized. In other three
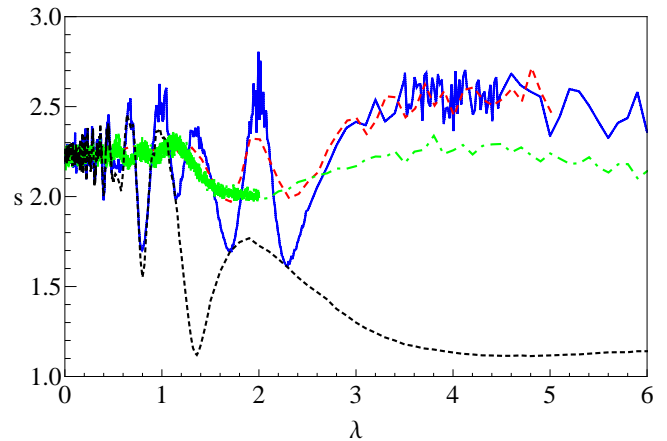

FIG. 11: Ratio $s(\lambda)$ vs. wavelength λ for $Q_\nu = 0.25$ and the stack length $N = 10^3$. Solid and dashed curves are for the RID H-stack and H-stack with $Q_d = 0.2$, respectively. The middle dashed-dotted curve is for an M-stack with $Q_d = 0.25$, and the bottom dotted line is for a RID M-stack.
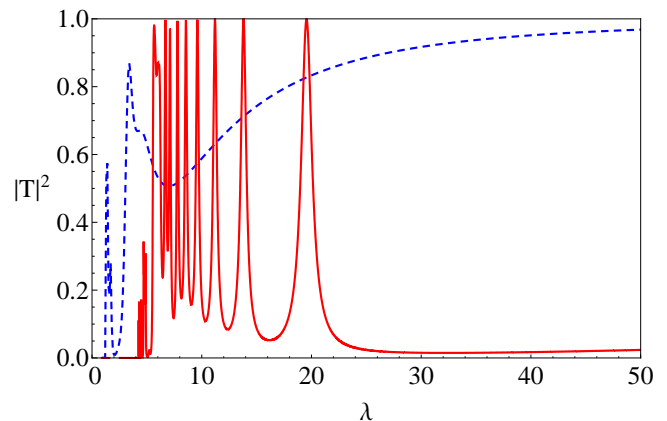

FIG. 12: Single realization transmittance $|T|^2$ vs wavelength λ for RID M-stacks with $Q_\nu = 0.25$ and $Q_d = 0$ for $N = 10^5$ layers (solid line) and $N = 10^3$ layers (dotted line).

cases, however, $s(\lambda) \gtrsim 2$, which means that the localization takes place even in a comparatively short stack.

Thus, there are two possibilities to introduce transmission resonances. The first is to increase the length of the stack. Fig. 12 displays the RID M-stack transmittance $|T|^2$ for a single realization as a function of λ for two lengths: $N = 10^5$ (solid line) and $N = 10^3$ (dotted line). It is readily seen that while there are no resonances in the shorter stacks, they do appear in the longer samples. The second way to generate transmission resonances is to introduce thickness disorder. To demonstrate this, we plot in Fig. 13 the transmittance of a single M-stack with both thickness and refractive index disorder. It clearly shows that while the RID M-stack is too short to exhibit transmission resonances at $\lambda > 3$, at the M-stack with thickness disorder, resonances emerge
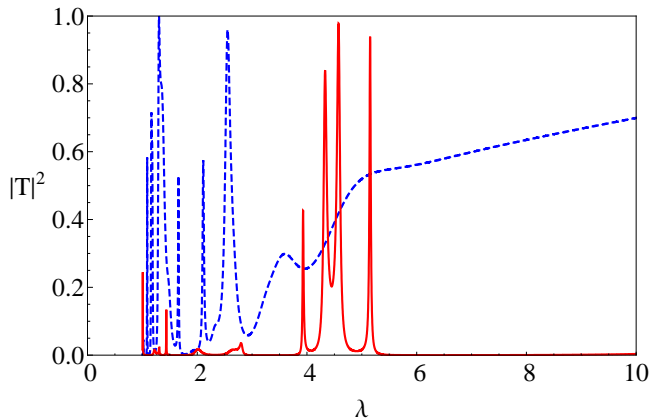
FIG. 13: Single realization transmittance $|T|^2$ vs λ for M-stack of $N = 10^3$ layers with $Q_\nu = 0.25$. Solid line corresponds to an M-stack with $Q_d = 0.2$, and the dashed line to M-stack with no thickness disorder, i.e., $Q_d = 0.0$.

at longer wavelengths.

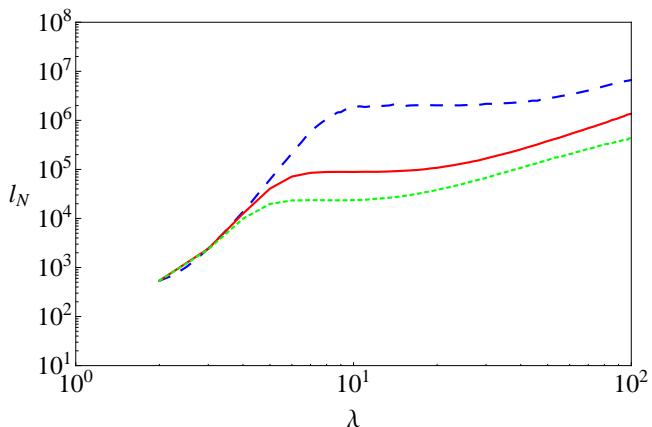### 3. Effects of the thickness disorder and uncorrelated paring

FIG. 14: Localization length l vs. wavelength λ for a M-stack with $Q_\nu = 0.25$ and Q_d=0.001, 0.005, and 0.01 (from top to bottom).

Here, we analyze the effect of thickness disorder on λ^6-anomaly — that is the λ^6 dependence of the transmission length. In Fig. 14, we plot the transmission length l_N for an M-stack with fixed refractive index disorder ($Q_\nu = 0.25$) for various values of the thickness disorder. It is evident that the transmission length changes from $l \propto \lambda^6$ to the classical dependence $l \propto \lambda^2$ as the thickness disorder increases from $Q_d = 0.001$ (top curve) to $Q_d = 0.01$ (bottom curve). In all cases, the number of layers $N = 10^8$ is longer than the transmission length, guaranteeing that Fig. 14 represents the genuine local-
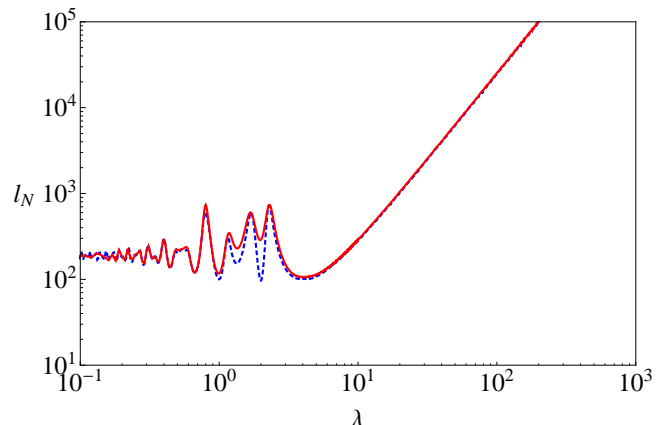
ization length l.

FIG. 15: Transmission length l_N vs. wavelength λ for the H-stack with R-layers (dashed line) and an M-stack (solid line) in which each subsequent layer is chosen with equal probability to be of R- or L-type. The stacks in both calculations are of the same size, $N = 10^4$.

We have also found that the anomalous dependence $l \propto \lambda^6$ (or with higher power) is extremely sensitive to the alternation of left- and right-handed layers. To demonstrate this, we consider an M-stack of length $N = 10^4$, in which each subsequent layer is chosen with equal probability to be either right- or left-handed. Figure 15 shows the transmission length spectrum for this case, which is almost the same for both the H-stacks and M-stacks. The only difference is a fairly modest suppression of localization, which occurs within the wavelength interval $0.5 < \lambda < 2.5$. This result confirms that it is the additional correlation between left-handed and right-handed layers in the alternating stack which is responsible for the suppression of localization.

C. Effects of losses

In this section, we study the transmission through layered media with absorption, which is characteristic of real meta-materials. In this case, the exponential decay of the field is due to both Anderson localization and absorption [27, 33], and in some limiting cases, it is possible to distinguish between these contributions.

For an M-stack with weak fluctuations of the refractive index and weak thickness disorder, WSA theory in the limits of short or long waves leads to the well-known formula

$$\frac{1}{l_{\text{att}}} = \frac{1}{l_N} + \frac{1}{l_{\text{abs}}},$$

where l_N is the disorder-induced transmission length in the absence of absorption, and the absorption length is

$$l_{\text{abs}} = \frac{\lambda}{2\pi\sigma}. \tag{63}$$

For short wavelengths, l_N^{-1} is constant given by Eqs (30), (34) and (36), while for long wavelengths, in either the localized or ballistic regimes, its contribution is proportional to λ^{-2} and thus is negligibly small in comparison with the contribution due to losses, which is always proportional to λ^{-1}. Accordingly, at both short and long wavelengths, the attenuation length coincides with the absorption length (63), with disorder contributing significantly to the attenuation length only in some intermediate wavelength region, provided that the absorption is sufficiently small.
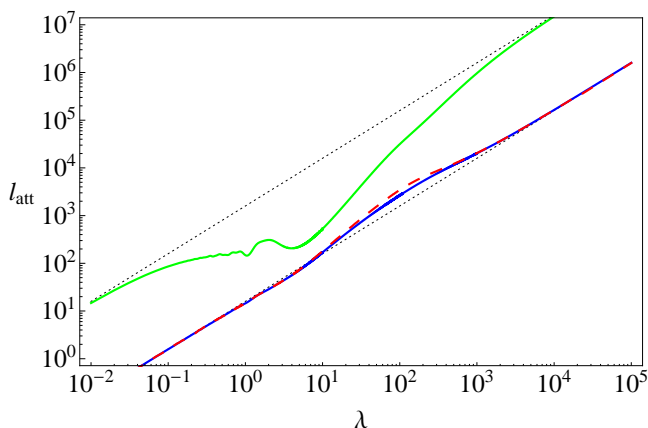

FIG. 16: Attenuation length l_{att} and absorption length l_{abs} vs. wavelength λ for an M-stack with disorder $Q_\nu = 0.25$, $Q_d = 0.2$ and length $N = 10^4$. The upper solid line displays the (identical) simulation and WSA results for $\sigma = 10^{-4}$; the lower solid line presents numerical results for while the dashed line displays WSA results for the same absorption value. Absorption lengths (63) for both $\sigma = 10^{-4}$ and $\sigma = 10^{-2}$ are shown by dotted straight lines.

The results of the numerical calculations shown in Fig. 16 completely confirm the theoretical predictions presented above. For weak absorption $\sigma = 10^{-4}$, the direct simulation and WSA theory give exactly the same result (solid curve in Fig. 16). Over a reasonably wide wavelength range, $10^{-1} \lesssim \lambda \lesssim 10^3$, disorder contributes significantly to the attenuation. For such a stack, the characteristic wavelengths are $\lambda_1(N) = 47$ and $\lambda_2(N) = 265$, implying that the contribution of disorder is significant in all regions, from the short wavelength part of the localized regime to the long wavelength ballistic region. Due to the losses, however, there are fewer oscillations evident in the transmission length spectrum than in the lossless case of Fig. 2.

For stronger absorption, $\sigma = 10^{-2}$, the wavelength range, over which disorder contributes to the attenuation is reduced, as well as the relative value of the contribution itself. The agreement between the numerical simulations and the WSA calculations is reasonable.

V. CONCLUSIONS

We have studied the transmission and localization of classical waves in one-dimensional disordered structures composed of alternating layers of left- and right-handed materials (M-stacks) and compared this to the transport in homogeneous structures composed of different layers of the same material (H-stacks). For weakly scattering layers and general disorder, where both refractive index and thickness of each layer is random, we have developed an effective analytical approach, which has enabled us to calculate the transmission length over a wide range of input parameters and to describe transmission through M- and H-stacks in a unified way. All theoretical predictions are in excellent agreement with the results of direct numerical simulations.

There are remarkable distinctions between transmission and localization properties of the two types of stacks. When both types of disorder (refractive index and layer thickness) are present, the transmission length of a H-stack in the localized regime coincides with the reciprocal of the Lyapunov exponent, while for M-stacks these two quantities differ by a numerical prefactor. This is quite surprising and, to the best of our knowledge, it is the first time that a system where such a difference exists has been discovered.

It is shown that the stacks of M- and H-type manifest quite different behaviour of the transmission length as a function of wavelength. This difference is most pronounced in the long wavelength region. In the localized regime, stacks of both types are strongly disordered and reflect the incident wave almost entirely. In the ballistic regime, where stacks are almost transparent, the transport properties of H-stacks and M-stacks are markedly different. H-stacks, over the moderately long wavelength ballistic region, and M-stacks, over the entire long wavelength region, are weakly scattering disordered structures. In the extremely long wavelength ballistic region, the H-stack becomes effectively uniform — a regime which is absent for M-stacks because of the intrinsic non-uniformity caused by the alternating nature of the structure. The crossover regions between different regimes are comparatively narrow.

The transmission length for a single realization is non-random in the localized regime for both types of stacks, and in far ballistic regime for the H-stack. In the case of M-stacks, the transition from the localized to the ballistic regime is accompanied by a change in the wavelength dependence of the transmission length. In contrast, for H-stacks, the corresponding change occurs in the vicinity of the transition from the weak scattering (near ballistic) regime to the uniform (far ballistic) regime. The crossover regions between the different regimes again are comparatively narrow.

In M-stacks with only refractive-index disorder, Anderson localization is substantially suppressed, and the localization length grows with increasing wavelength much faster than the classical square law dependence. The crossover region becomes significantly wider, and transmission resonances occur in much longer stacks than in the corresponding H-stacks.

The effects of absorption on the one-dimensional transport and localization have also been studied, both analytically and numerically. In particular, it has been shown that the crossover region is particularly sensitive to losses, so that even small absorption suppresses noticeably the oscillations of the transmission length in the frequency domain.

VI. ACKNOWLEDGMENTS

APPENDIX: UNIFORM DISTRIBUTION OF FLUCTUATIONS

If the fluctuations $\delta_j^{(\nu)}$ and $\delta_j^{(d)}$ are uniformly distributed in the intervals $[-Q_\nu, Q_\nu]$ and $[-Q_d, Q_d]$ respectively, and absorption is the same in all slabs ($\sigma_j = \sigma$), the transmission, localization, and ballistic lengths given by Eqs. (22)-(26) can be calculated explicitly in the weak scattering approximation. The results are:

$$\langle t^2 \rangle = \frac{1}{8ikQ_\nu Q_d}\left[Ei(i\Delta_+ n_+) - Ei(i\Delta_- n_+)\right.$$
$$\left. - Ei(i\Delta_+ n_-) + Ei(i\Delta_- n_-)\right], \quad \text{(A.1)}$$

$$\langle r \rangle = \frac{e^{i\Delta_+(1+i\sigma)}}{8ikQ_d}\left[\frac{\sin(\Delta_+ Q_\nu)}{\Delta_+ Q_\nu} - \frac{\sin(\Delta_- Q_\nu))}{\Delta_- Q_\nu}\right] +$$
$$+ \frac{i\sigma}{2}(\langle t^2 \rangle - 1) + \frac{1+i\sigma}{2}\langle t^2 \rangle, \quad \text{(A.2)}$$

$$\langle |r|^2 \rangle = 2k\sigma + \frac{Q_\nu^2}{6} - \frac{\sigma^2}{4}(\mathrm{Re}\langle t^2 \rangle - 1)$$
$$+ 2\sigma\mathrm{Im}\langle r \rangle - 2\mathrm{Re}(H_1 + H_2). \quad \text{(A.3)}$$

Here,

$$\Delta_\pm = 2k(1 \pm Q_d),$$
$$n_\pm = 1 \pm Q_\nu + i\sigma,$$
$$H_1 = \frac{e^{i\Delta_+(1+i\sigma)}}{8kQ_\nu Q_d \Delta_+^2}[1 + i\Delta_+(1+i\sigma)\sin(\Delta_+ Q_\nu) -$$
$$- \Delta_+ Q_\nu \cos(\Delta_+ Q_\nu)]$$
$$+ \frac{i(1+i\sigma)^2}{16kQ_\nu Q_d}[Ei(i\Delta_+ n_-) - Ei(i\Delta_+ n_+)],$$

where H_2 is obtained from H_1 by the replacement of Δ_+ by Δ_-, and $Ei(z)$ is the integral exponential function given by [IntExp]

$$Ei(z) = -\int_{-z}^{\infty} \frac{e^{-t}}{t} dt.$$

[1] V. G. Veselago, Sov. Phys. Usp. **10**, 509 (1968).
[2] J. B. Pendry, Phys. Rev. Lett. **85**, 3969 (2000).
[3] P. Marcos, C.M. Soukoulis, *Wave propagation from electrons to photonic crystals and left-handed materials*, (Princeton university press, Princeton,2008).
[4] K.Yu. Bliokh, and Yu. P. Bliokh, Physics - Uspekhi **47**, 393 (2004) [Usp. Fiz. Nauk **174**, 439 (2004)].
[5] C. Caloz and T. Ito, Proceedings of IEEE **93**, 1744 (2005).
[6] V.M. Shalaev, Nature Photonics **1**, 41 (2007).
[7] D. Schurig, J. Mock, B. Justice, S. Cummer, J. Pendry, A. Starr, and D. Smith, Science **314**, 977 (2006).
[8] J. Kästel and M. Fleischhauer, Phys. Rev. A **71**, 011804 (2005).
[9] Y. Yang, J. Xu, H. Chen, and S. Zhu, Phys. Rev. Lett. **100**, 043601 (2008).
[10] L.G. Wang, H. Chen, and S.-Y. Zhu, Phys. Rev. B **70**, 245102 (2004).
[11] M. V. Gorkunov, S.A. Gredeskul, I.V. Shadrivov, and Yu.S. Kivshar, Phys. Rev. E **73**, 056605 (2006).
[12] P.W. Anderson, Phys. Rev. **109**, 1492 (1958).
[13] S. John, Phys. Rev. Lett., **53**, 2169 (1984).
[14] I.M. Lifshits, S.A. Gredeskul, and L.A. Pastur, *Introduction to the Theory of Disordered Systems* (Wiley, New York 1987), and references therein.
[15] P. Sheng *Scattering and localization of classical waves in random media* (Singapore: World Scientific 1991).
[16] V. D. Freilikher and S.A. Gredeskul, *Progress in Optics* **30**, 137 (1992).
[17] S.A. Gredeskul, A.V. Marchenko, and L.A. Pastur, *Surveys in Applied Mathematics*, v. 2 (Plenum Press, New York 1995), p. 63.

[18] P. Sheng, *Introduction to Wave Scattering, Localization, and Mesoscopic Phenomena* (Springer-Verlag, Heidelberg, 2006).

[19] N. Mott and Twose, Adv. Phys. **10**, 107 (1961).

[20] F. M. Israilev, N.M. Makarov, E. J. Torres-Herrera, arXiv:0911.0966v1 [cond-mat.mes-hall], 5 Nov. 2009.

[21] Y. Dong and X. Zhang, Phys. Lett. A **359**, 542 (2006).

[22] A.A. Asatryan, L.C. Botten, M.A. Byrne, V.D. Freilikher, S.A. Gredeskul, I.V. Shadrivov, R.C. McPhedran, and Yu.S. Kivshar, Phys. Rev. Lett. **99**, 193902 (2007).

[23] V. Baluni and J. Willemsen, Phys. Rev. A **31**, 3358 (1985).

[24] E.M. Nascimento, F.A.B.F. de Moura, and M.L. Lyra, Optics Express **16**, 6860 (2008).

[25] P. Han, C.T. Chan, and Z.O. Zhang, Phys. Rev. B **77**, 115332 (2008).

[26] C. M. de Sterke, and R.C. McPhedran, Phys. Rev. B **47**, 7780 (1993).

[27] A.A. Asatryan, N.A. Nicorovici, L.C. Botten, C. M. de Sterke, P.A. Robinson, and R.C. McPhedran, Phys. Rev. B **57**, 13535 (1998).

[28] G. A. Luna-Acosta, F.M. Izrailev,N.M. Makarov, U. Kuhl, and H.-J. Stockman, Phys. Rev. B **80**, 115112 (2009).

[29] S.M. Rytov, Yu.A. Kravtsov, and V.I. Tatarskii, *Principles of Statistical Radiophysics* (Springer, Berlin, 1987).

[30] I. M. Lifshitz and V. Ya. Kirpichenkov, Sov. Phys. JETP **50**, 499 (1979) [Zh. Eksp. Teor. Fiz. **77**, 989 (1979)].

[31] M. Ya. Azbel and P. Soven, Phys. Rev. B **27**, 831 (1983).

[32] K.Yu. Bliokh, Yu.P. Bliokh, V. Freilikher, S. Savelïev, and F. Nori, Rev. Mod. Phys. **80**, 1201 (2008).

[33] V. Freilikher, M. Pustilnik, and I. Yurkevich, Phys. Rev. B **50**, 6017 (1994).

[34] V. Freilikher, B. Liansky, I. Yurkevich, A. Maradudin, A. McGurn, Phys. Rev. E 51, 6301 (1995)